



COB-2021-0207

Flow and Leakoff in a Hydraulic Fracture Using the Finite Volume Method

Keveen R. E. Tenereli

Hermínio T. Honório

Clovis R. Maliska

Universidade Federal de Santa Catarina

ktenereli@gmail.com, herminio@sinmec.ufsc.br, maliska@sinmec.ufsc.br.

Abstract. Hydraulic fracturing is an important stimulation technique mainly applied to tight reservoirs. It consists of injecting a fracturing fluid at high pressure through a well with the intention of initiating and propagating fractures. These fractures ultimately increase the formation permeability and thus the well productivity. The present work focuses on the numerical modeling of the fluid flow through the fracture and the surrounding porous rock, where a rigid solid skeleton is assumed. The fluid flow inside the fracture is considered to be one-dimensional and it is mathematically modeled in two different ways. In the first model, the Navier-Stokes equations are solved for both the pressure and velocity fields. Alternatively, a cubic law, obtained through the Poiseuille solution for a flow between parallel plates, is employed to evaluate velocities in the mass conservation equations, so the pressure field is the only unknown. These two models carry different assumptions and simplifications, so a comparison is carried out in terms of accuracy and computational cost. The fracture (flow) models are discretized through the Conventional Finite Volume Method (FVM) in a one-dimensional grid. For the fluid flow through the surrounding porous medium, on the other hand, the Element based Finite Volume Method (EbFVM) is employed for the discretization of the mass conservation equation in two-dimensional unstructured grids. The two physical processes (i.e. fluid flow inside fracture and porous medium) are coupled through the fluid exchange between the channel and the rock formation, the so called leakoff. The numerical strategy for treating the coupling between these two physical processes is described in details. The results show that the two models for fluid flow inside fractures produce almost the same results in most practical situations. Discussions and physical interpretations of the results are also provided in this work. Finally, the coupling strategy is shown to provide physically consistent results.

Keywords: Hydraulic fracturing, Finite Volume Method, Unstructured grids

1. INTRODUCTION

The process of hydraulic fracturing consists of coupled physical phenomena, such as the flow inside the fracture and the leak-off to the rock, which are the focus of this work. Figure 1 shows a fracture with a variable opening D , in the longitudinal direction s , with a flow q_i at fracture entrance and the leak-off to the rock medium q_l normal to the fracture faces.

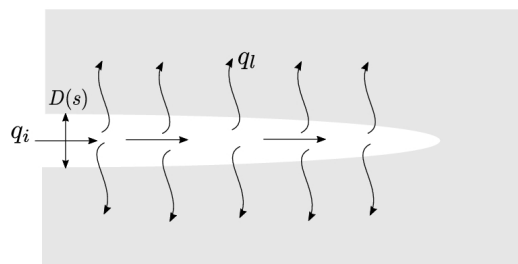


Figure 1: Representation of fracture flow and leakoff.

The flow inside the fracture is usually modeled using the local cubic law, a mass conservation equation derived from Poiseuille's equation for laminar, fully developed flow between parallel plates, which has experimental confirmation for fractures (Whiterspoon, 1980).

As for the fluid exchange between the fracture and the rock, the leak-off, is caused by the pressure gradient between these two domains and is usually modeled using Carter's law (Howard *et al.*, 1957). This model assumes that the hydraulic head, the difference between the pressure of the fluid in the fracture and the pore pressure of the reservoir, is constant in time (Mitchell *et al.*, 2007) and employs a constant fluid loss, typically obtained from experimental results (Lecampion *et al.*, 2018). Later works have used variations of Darcy's law to model the leak-off and the fluid flow porous skeleton

such as the works of (Simoni and Secchi, 2003; Carrier and Granet, 2012; Manzoli *et al.*, 2019; Manchanda *et al.*, 2020). The work of Manchanda *et al.* (2020), in particular, uses the Finite Volume Method for discretizing the model equations.

In terms of numerical methods, the Finite Element Method is traditionally used for the elasticity equations of the rock mechanics as well as for the fluid equations. For the latter, the Finite Volume and the Finite Difference Methods are also employed (Lecampion *et al.*, 2018).

This work proposes to solve the flow inside an already opened fracture using the local cubic law, as well as an alternative model obtained through the one-dimensional momentum equation, the well known Navier-Stokes equation, with a friction factor to account for the diffusive effect of the fracture wall, with a coupled mass conservation. The porous medium flow model is discretized using the Element based Finite Volume Method, and a coupling algorithm for the leak-off is presented.

The traditional and proposed mathematical formulations are presented in Sec. 2. In Sec. 3, the numerical model, as well as the proposed coupling algorithm for the leak-off, are shown. In Sec. 4, the results for the flow inside and outside the fracture are presented, as well as comparisons between both fracture flow models and results with both structured and unstructured meshes. Finally, a few closing remarks are presented.

2. MATHEMATICAL MODEL

The single phase flow of a slightly compressible fluid in a porous medium is given by the mass balance equation in conjunction with Darcy's law, that is,

$$\phi c_f \frac{\partial p}{\partial t} - \nabla \cdot \left(\frac{k}{\mu} \nabla p \right) = 0, \quad (1)$$

in which ϕ is the rock porosity, c_f is the fluid compressibility, p is the pore pressure, μ is viscosity and k represents the medium absolute permeability. Notice that gravitational effects are neglected from Eq. (1) and the permeability tensor is considered to be isotropic.

The flow inside the fracture is considered to be one dimensional and governed by the mass conservation equation with the velocity along its length obtained by the solution of Poiseuille's flow between parallel plates (Lecampion *et al.*, 2018). The fluid loss (leakoff) is defined as the coupling parameter between the fracture and the rock in this work, it is then modeled using Darcy's law. This equation for a slightly compressible fluid is,

$$D c_f \frac{\partial p}{\partial t} + \frac{\partial}{\partial s} \left(-\frac{D^3}{12\mu} \frac{\partial p}{\partial s} \right) - \frac{k}{\mu} \frac{\partial p}{\partial n} \Big|_{\text{sup}} - \frac{k}{\mu} \frac{\partial p}{\partial n} \Big|_{\text{inf}} = 0, \quad (2)$$

where D is the fracture opening, and s and n denote the longitudinal and normal direction to the fracture flow. The last two terms represent the pressure gradient evaluated at both fracture faces – superior and inferior – that produce the leak-off.

The alternative model for the flow inside the fracture presented here is based on the one-dimensional Navier-Stokes equation with a friction factor. This friction factor models the head loss of the flow, and its values are also obtained from Poiseuille's solution for parallel plates. By the presence of diffusive and advective terms, it is expected to offset some of the accompanying simplifications of this factor. The equations can be written as,

$$D \frac{\partial}{\partial t} (uD) + \frac{\partial}{\partial s} (uuD) = -\frac{\partial}{\partial s} (pD) + \frac{\mu}{\rho} \frac{\partial}{\partial s} \left(2 \frac{\partial}{\partial s} (uD) \right) - f u^2, \quad (3)$$

$$\frac{\partial}{\partial s} (uD) - \frac{k}{\mu} \frac{\partial p}{\partial n} \Big|_{\text{sup}} - \frac{k}{\mu} \frac{\partial p}{\partial n} \Big|_{\text{inf}} = 0, \quad (4)$$

where u is the velocity in the s direction, ρ is the fluid density and f is the friction factor (Bejan, 2004), computed as

$$f = \frac{12\mu}{\rho u D}, \quad (5)$$

for parallel plates.

3. NUMERICAL MODEL

The element based finite volume method (EbFVM) is employed to discretize the equation for fluid flow in the porous medium, Eq. (1). As a finite volume method, it is inherently conservative and by being based on elements, it allows the use of unstructured grids, providing greater flexibility, especially for irregular geometries.

The EbFVM is a *cell-vertex* method, so the center of the control volumes coincides with the vertices of the elements. Each element is then divided into sub-elements or sub-volumes. The union of sub-volumes associated with a particular

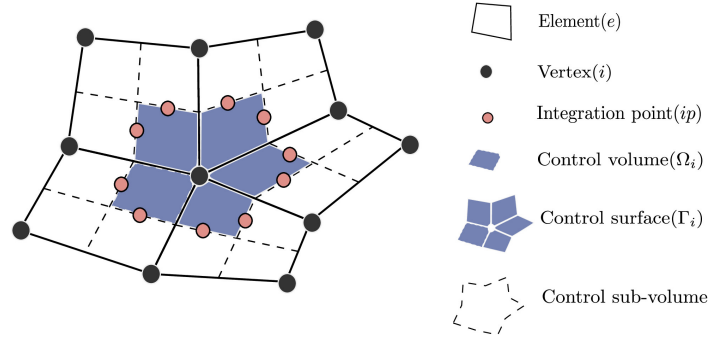


Figure 2: Geometrical entities of the EbFVM.

vertex produces the control volume Ω_i . The faces created by this division compose the control surface Γ_i , and each face has an integration point at its centroid. These geometrical entities can be observed in Fig. 2. The discretized equation for the flow in the porous medium is obtained through the EbFVM by integrating over a time step Δt and over a general control volume Ω_i . As shown in (Honório *et al.*, 2018), the resulting equation can be represented as,

$$\phi c_f \Delta \Omega_i \frac{p_i}{\Delta t} + \sum_{ip \in \Gamma_i} \left(-s_{ip}^T \frac{\mathbf{k}^e}{\mu} \mathbf{B}_{ip} \mathbf{p}^e \right) = \mathbf{b}_i^p, \quad (6)$$

where s_{ip} is the area vector and \mathbf{B}_{ip} is the gradient operator, defined as the matrix of shape functions derivatives $\nabla \mathbf{N}^T$. At last, the source term \mathbf{b}_i^p is given by,

$$\mathbf{b}_i^p = \phi c_f \Delta \Omega_i \frac{p_i^o}{\Delta t}, \quad (7)$$

the superscript o in the source term refers to "old" and indicate the variable computed in the previous time level.

The equations for flow inside the fracture are obtained through the Conventional Finite Volume Method (FVM), which is a cell-center method. Similar to the previous discretization, this is done by integrating the differential equation over a control volume and a time step. The derivatives are then approximated using central difference. Figure 3 shows the central control volume P and its neighbors, where N and S , North and South, respectively, are elements of the porous medium W and E , West and East, are fracture volumes.

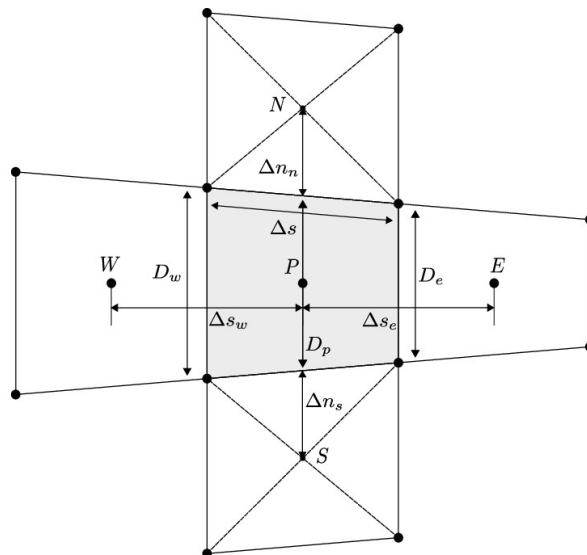


Figure 3: Elementary volume and neighbors.

The discretized equation for the model based on the Poiseuille velocity, Eq. (2) is then,

$$\frac{\Delta s}{\Delta t} D_{PCf} (p_P - p_P^o) = \frac{D_e^3}{12\mu} \frac{p_E - p_P}{\Delta s_e} - \frac{D_w^3}{12\mu} \frac{p_P - p_W}{\Delta s_w} + \frac{k}{\mu} \frac{p_N - p_P}{\Delta n_n} \Delta s + \frac{k}{\mu} \frac{p_S - p_P}{\Delta n_s} \Delta s. \quad (8)$$

The fracture openings are evaluated at the volume's faces and center, expressed respectively by D_e , D_w and D_p , this notation is also used for the pressures and the distance between volumes Δs . The characteristic length Δn represents the

distance between the fracture's faces to the center of the element to its north and south, where the medium pressure is located.

For the model based on Navier-Stokes, Eq. (3) and Eq. (4), a one dimensional discretization is also required, this time, in a staggered grid, where the velocity u is located in the faces of the volume and the pressure p is located in the volume's center (Maliska, 2004).

$$\frac{\Delta s}{\Delta t} D_p (u_P - u_P^o) + \dot{m}_e u_e - \dot{m}_w u_w = -(p_e - p_w) D_p + 2\mu \frac{u_E - u_P}{\Delta s_e} D_e - 2\mu \frac{u_P - u_W}{\Delta s_w} D_w - \Delta s \left(\frac{12\mu u_P}{D_P} \right), \quad (9)$$

here the lowercase w and e denote the faces of the volumes W and E respectively.

The *Upwind* interpolation function is used for the flow equation in the fracture, as

$$\begin{aligned} u_e &= u_P \quad \text{and} \quad u_w = u_W \quad \text{if} \quad u > 0; \\ u_e &= u_E \quad \text{and} \quad u_w = u_P \quad \text{if} \quad u < 0. \end{aligned} \quad (10)$$

Using the same discretization process, the mass conservation equation, Eq. (4), is given by,

$$\dot{m}_e - \dot{m}_w - p_P \left[\Delta s \frac{k}{\mu} \left(\frac{1}{\Delta n_s} + \frac{1}{\Delta n_n} \right) \right] + p_N \frac{k}{\mu} \frac{\Delta s}{\Delta n_n} + p_S \frac{k}{\mu} \frac{\Delta s}{\Delta n_s} = 0. \quad (11)$$

3.0.1 LEAK-OFF COUPLING

As previously mentioned, the coupling parameter between the domains is the leak-off, given by Darcy's law, that is,

$$q_{\text{leakoff}} = \frac{k}{\mu} \frac{p_f - p_m}{\Delta n} \Delta s, \quad (12)$$

where p_f is the pressure in the fracture and p_m the porous medium pressure at the adjacent element. The general solution and coupling between the flow in the fracture and the flow in the porous media will be performed by the subsequent algorithm:

1. With the initial pressure field, solve the fracture flow to obtain p_f ;
2. Calculate leakoff for both fracture faces using the calculated p_f and the initial p_m ;
3. Apply the leakoff as a Neumann boundary condition on the fracture faces using Eq. (12), solve the porous media flow to obtain a new p_m ;
4. With p_m calculated at the previous step, return to the first step to obtain a new p_f ;
5. Repeat the process until a predetermined criteria is satisfied;
6. Advance the time level.

Given that the variables on the unstructured mesh are located at each element vertex, the elements where the Neumann boundary condition has to be applied will have associated to it three or four variables – depending on the nature of the elements, to each variable on the adjacent fracture volume. Figure 4 shows how the mesh for the fracture, colored blue, and the mesh for the porous medium connect, in this example the elements are composed of four vertices.

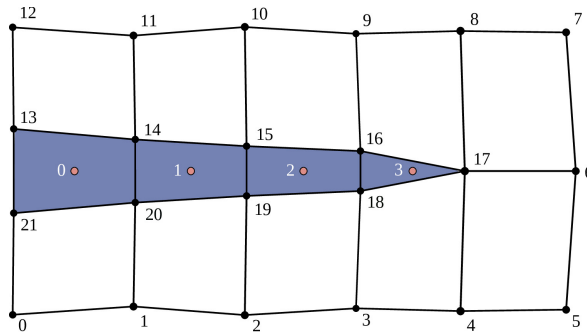


Figure 4: Illustration of fracture and porous medium meshes.

To solve this problem the mean value of the pressures of the element is used. Using Figure 4, the element to the north of volume 1, would have a mean pressure p_m composed of the values of nodes 10, 11, 14 and 15, given the distance to its geometric center Δn_n . The leak-off over the boundary would be, then, computed using this average pressure p_m and the fracture pressure p_f at volume 1.

4. RESULTS AND DISCUSSION

The flow inside the opened fracture channel together with the leak-off to the porous medium and the subsequent flow is simulated using the two models previously mentioned, the mass conservation equation with velocity based on Poiseuille's solution, Eq. (2), and the model based on Navier-Stokes equations, Eq. (3) and Eq. (4), together with the model for fluid flow in the porous medium, Eq. (1).

The boundary conditions used are: Prescribed pressure at the fracture inlet of 5 MPa, zero pressure in the north, south and east boundaries of the porous medium. The west boundary of the rock is taken to be impermeable as is the fracture tip. The initial pressure over both domains is taken to be zero as well. These boundary conditions can be seen in Fig 5.

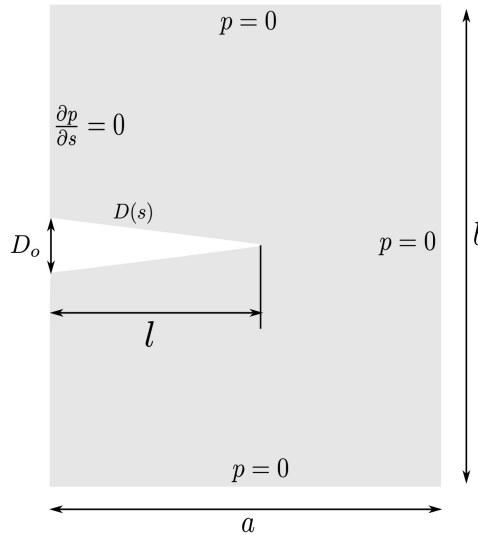


Figure 5: Problem's domain and boundary conditions.

Table 1 shows the geometrical values used throughout this work. As it can be seen from Fig. 5, the opening of the fracture varies linearly through its length as to have zero cross-section at the fracture tip.

Geometric Parameters	Values
Fracture Initial Opening (D_o), m	0.0005
Fracture Length (l), m	10
Medium Width (a), m	18
Medium Height (b), m	12
Medium Depth, m	1

Table 1: Geometric parameters for fracture and medium.

Table 2 shows the physical properties used in the simulations. The fracturing fluid is considered to be slightly compressible.

Physical Constant	Values
Density (ρ), kg/m^3	1000
Fluid Compressibility (c_f), $1/Pa$	5×10^{-10}
Viscosity (μ), $Pa \cdot s$	0.001
Porosity (ϕ)	0.2
Absolute Permeability (k), m^2	5×10^{-15}

Table 2: Physical properties for the simulation.

The simulation is run until a steady state-regime is reached, using a time step of $\Delta t = 0.1s$. The flow in the porous medium is solved using an in-house Python library named PyEFVLib, developed for EbFVM applications. The flow inside the fracture is solved using a code developed by the authors and integrated using the previously mentioned algorithm. For the results presented here, the fracture was discretized with eighty control volumes. The solutions for both domains (porous medium and fracture) are obtained by LU decomposition. The convergence criteria, both for the time progression as well as for the leak-off coupling loop is of 10^{-5} .

Figure 6 shows the results for both pressure and velocity inside the fracture for three different values of permeability, 1×10^{-15} , 5×10^{-15} and $1 \times 10^{-14} \text{ m}^2$. For each permeability, both fracture flow models are used, the local cubic law model, referenced here as Poiseuille, and the model with a momentum equation, denoted as Navier-Stokes. It should be also noted that as the velocity is not explicitly solved for in the cubic law model, the values have to be computed afterward using the pressure gradient obtained. The same does not apply to the Navier-Stokes model, since a staggered arrangement of variables is adopted and the velocity and pressure are calculated.

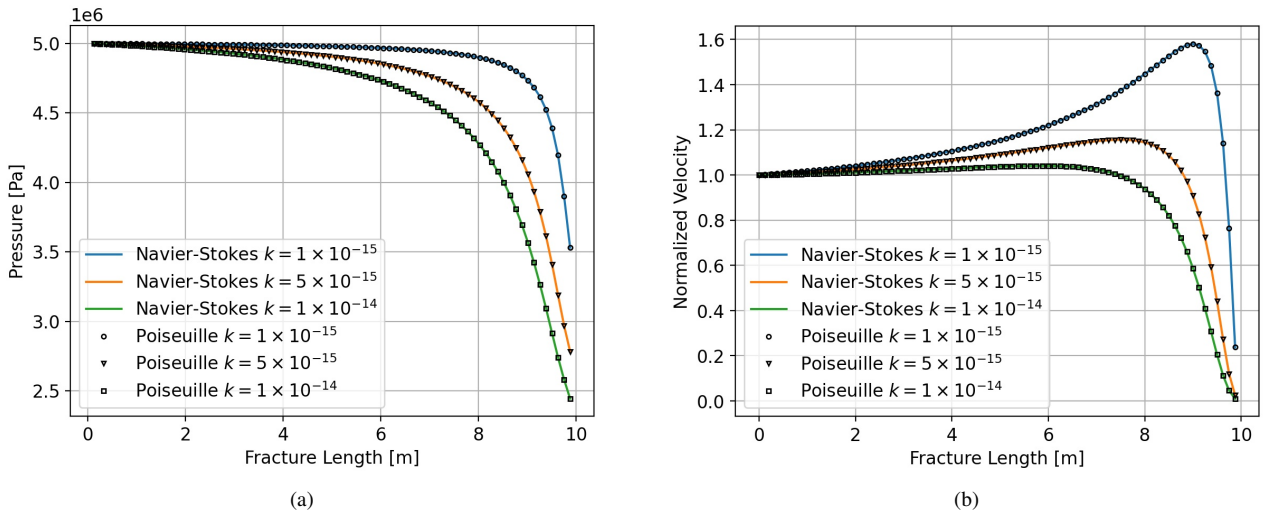


Figure 6: (a) Pressure profiles for both flow models; (b) Velocity profiles for both flow models.

As it can be observed in Fig. 6, both models provide virtually the same results in all situations. The differences between the behavior of each result are due to the effect of fluid loss from the leak-off. This leak-off causes the decrease of the pressure along the length of the fracture, and with a larger value of permeability, this pressure loss is also larger. The fluid velocity increases due to mass conservation, as a reduced area implies a greater velocity so continuity can be satisfied. This becomes more apparent with a small enough leak-off. As the flow inside the fracture is reduced due to the fluid loss, the leak-off becomes more significant, allowing the velocity to decrease as well.

The next results presented here use the intermediate permeability value of $5 \times 10^{-15} \text{ m}^2$. In Figure 7(a) it can be seen that the pressure at the tip approaches the same pressure at the neighboring elements of the rock. This pressure at the elements, it should be noted, is the mean value of the pressures at the nodes that compose the element. In Figure 7(b) the leak-off profile for the fracture at the steady-state regime is shown. The leak-off increases, as the flow inside the fracture becomes smaller, this fluid exchange, in turn, results in a rise in pressure at the porous medium over the whole fracture length. As the fluid pressure inside the channel – especially close to the tip – is reduced, its values approach the pressure at the surrounding medium, Fig. 7(a), the leak-off then, starts to become increasingly smaller.

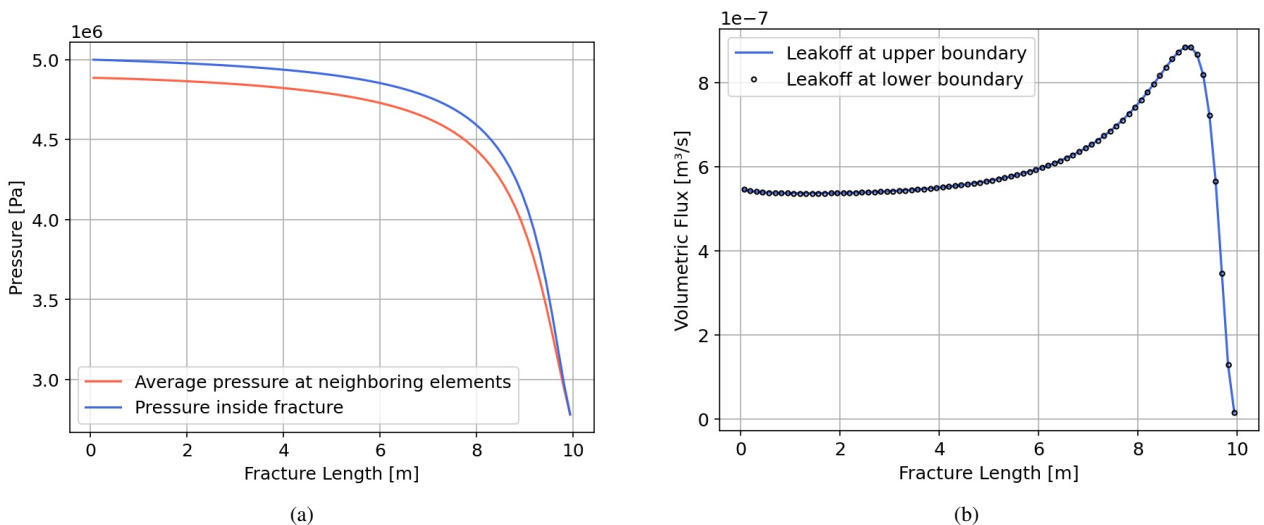


Figure 7: (a) Pressure profiles at neighboring elements and fracture; (b) Leakoff profile at fracture boundaries.

The dynamic between volumetric flow inside the fracture and leak-off can be observed in Fig. 8, where the competing

mechanism of fracture fluid flow and leak-off are shown. Given the existence of a leak-off, the volumetric flow inside the fracture naturally decreases along its length, due to mass conservation. This fluid loss is the leak-off to the surrounding medium. As so little fluid reaches the fracture tip, the volumetric flow approaches the boundary condition of zero.

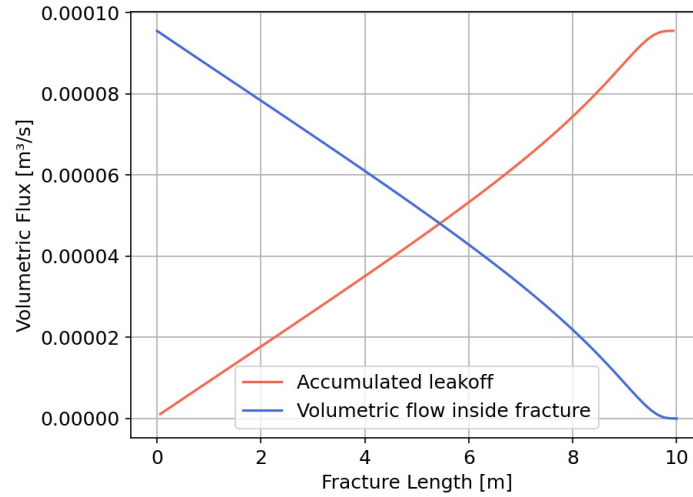


Figure 8: Volumetric flow and accumulated leakoff over fracture length

With the intent to further compare the two fracture flow models and find the situations where they differ, the fluid viscosity is progressively reduced, with the goal of minimizing the effects of the diffusive terms of the equations in benefit of the advective terms of the momentum equation, missing in the cubic law based model. The figure presented next, Fig. 9, correlates the relative error between the pressure profiles in the fracture with the local Reynolds number at the fracture entrance. This number is increased with the reduction of viscosity.

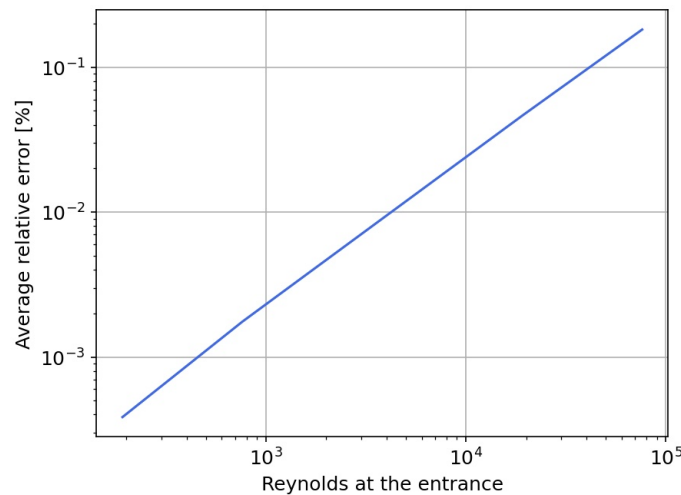


Figure 9: Relative error of pressure profiles with the increase of Reynolds number.

As shown, the relative error increases with the Reynolds number at the fracture entrance, as the advective forces start presenting a greater weight, compared to the diffusive forces, the models then, start to differ in a linear manner. The largest error, of approximately 1%, occurs with a local Reynolds number of over 10⁵, far above the usual threshold for laminar flow. In practical applications, the entrance Reynolds number is usually less than 5000 (Zia and Lecampion, 2017). At a Reynolds number of less than 10³ this error is less than 0.01%.

These results confirm that the use of the Navier-Stokes model is unnecessary for most hydraulic fracture applications. The Poiseuille model, with its greater simplifications, has an accurate performance for most cases at a far smaller computational cost, as this model solves only pressure instead of pressure and velocity, which is the case for the momentum equation, Eq. (3). For this grid size, the cubic law model has been observed to perform approximately 50% faster than the Navier-Stokes model.

4.1 Unstructured Grid

One of the advantages of the EbFVM method, besides being inherently conservative, is that it allows the use of unstructured meshes. In this section, the results for the fluid flow in the two-dimensional porous medium are presented, using both a structured mesh, that has been used for the results of this work so far, and an unstructured mesh. The problem simulated here is the same of the previous results.

This geometry is discretized - and the grid produced, using *Gmsh*, an open-source software for mesh generation. Illustrations for a structured and unstructured mesh are shown here in Fig. 10. These grids do not include the one-dimensional fracture mesh but identify the fracture's boundaries. Each of those boundaries will have associated to it the same number of elements as the fracture has volumes.

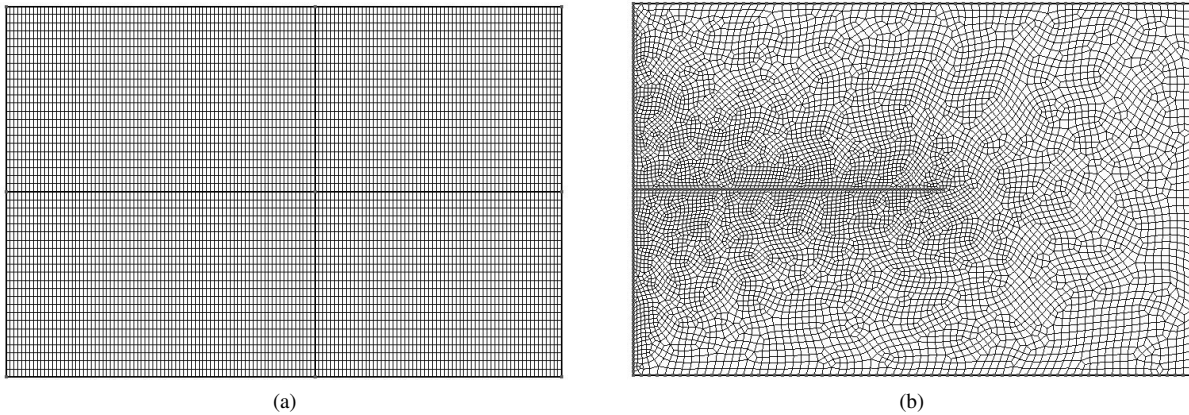


Figure 10: (a) Structured mesh for the two-dimensional porous domain with 6848 nodes; (b) Unstructured mesh for the two-dimensional porous domain with 7393 nodes.

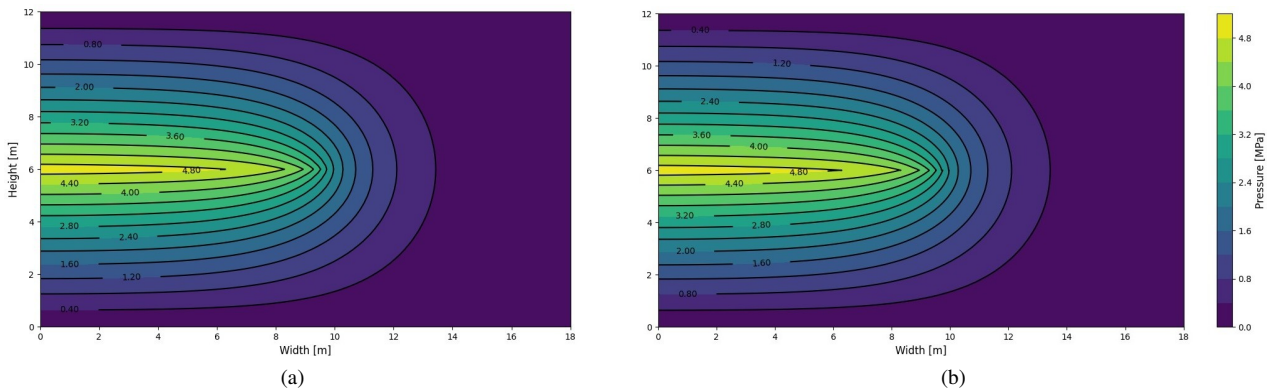


Figure 11: (a) Pressure field for structured mesh; (b) Pressure field for unstructured mesh .

The resulting pore pressure fields for both of these grids are shown in Fig. 11. The same general pressure field can be observed for the results of either mesh. Although it is illustrative, it shows the correct physical behavior. This confirms the use of the EbFVM for unstructured meshes. As expected, the resulting pressure is greater close to the fracture, and on the remaining boundaries, distant from fracture, the pore pressure approaches the prescribed value of zero. As the permeability of the rock is small, $5 \times 10^{-15} \text{ m}^2$, the penetration of fluid in the medium is small as well, with greater pressure gradients in the direction normal to the fracture faces due to the direction of the leak-off.

5. CONCLUSION

This paper presents results for fluid flow inside an opened hydraulic fracture, and the corresponding flow into the surrounding porous rock. These results were obtained using finite volume methods and, in particular, it was used the Element based Finite Volume Method for the solution of the flow in the porous medium. The results seem physically consistent.

One of the goals of this work was to propose an alternative model for fluid flow inside hydraulic fractures and, as so, this model carries different assumptions from the traditionally used models. It was observed, through comparisons, that the local cubic law and this alternative model produce close enough results for most practical cases, however, the computational cost for the new model is considerably greater. This can serve as justification for continuing the use of the

Poiseuille-based model. In the future, other tests may be performed with the intent of evaluating the limits of the model assumptions.

Another goal of this work was to propose an algorithm for the leak-off coupling, taking into account the numerical methods employed. The algorithm proposed in this paper uses Darcy's law for this coupling, instead of the traditional Carter's model and seems to produce the expected results for both the flow inside the fracture as well as the flow in the porous rock.

6. REFERENCES

- Adachi, J.I. and Detournay, E., 2002. "Self-similar solution of a plane-strain fracture driven by a power-law fluid". *International Journal for Numerical and Analytical Methods in Geomechanics*, Vol. 26, No. 6, pp. 579–604. ISSN 03639061. doi:10.1002/nag.213.
- Bejan, A., 2004. *Convection Heat Transfer*. Wiley New York, 3rd edition. ISBN 9780471271505,0471271500.
- Carrier, B. and Granet, S., 2012. "Numerical modeling of hydraulic fracture problem in permeable medium using cohesive zone model". *Engineering Fracture Mechanics*. ISSN 00137944. doi:10.1016/j.engfracmech.2011.11.012.
- Honório, H.T., Maliska, C.R., Ferronato, M. and Janna, C., 2018. "A stabilized element-based finite volume method for poroelastic problems". *Journal of Computational Physics*, Vol. 364, pp. 49–72. ISSN 10902716. doi: 10.1016/j.jcp.2018.03.010.
- Howard, G.C., Fast, C. *et al.*, 1957. "Optimum fluid characteristics for fracture extension". In *Drilling and production practice*. American Petroleum Institute.
- Lecampion, B., Bungler, A. and Zhang, X., 2018. "Numerical methods for hydraulic fracture propagation: A review of recent trends". doi:10.1016/j.jngse.2017.10.012.
- Maliska, C.R., 2004. *Transferência de Calor e Mecânica dos Fluidos Computacional*. Grupo Gen-LTC, 2nd edition.
- Manchanda, R., Zheng, S., Hirose, S. and Sharma, M.M., 2020. "Integrating Reservoir Geomechanics with Multiple Fracture Propagation and Proppant Placement". *SPE Journal*, , No. September 2019. ISSN 1086-055X. doi: 10.2118/199366-pa.
- Manzoli, O.L., Cleto, P.R., Sánchez, M., Guimarães, L.J. and Maedo, M.A., 2019. "On the use of high aspect ratio finite elements to model hydraulic fracturing in deformable porous media". *Computer Methods in Applied Mechanics and Engineering*, Vol. 350, pp. 57–80. ISSN 00457825. doi:10.1016/j.cma.2019.03.006.
- Mitchell, S.L., Kuske, R. and Peirce, A.P., 2007. "An asymptotic framework for finite hydraulic fractures including leak-off". *SIAM Journal on Applied Mathematics*, Vol. 67, No. 2, pp. 364–386. ISSN 00361399. doi:10.1137/04062059X.
- Simoni, L. and Secchi, S., 2003. "Cohesive fracture mechanics for a multi-phase porous medium". *Engineering Computations (Swansea, Wales)*, Vol. 20, No. 5-6, pp. 675–698. ISSN 02644401. doi:10.1108/02644400310488817.
- Whiterspoon, P.A., 1980. "Validity of Cubic Law for Fluid Flow in a Deformable Rock Fracture". Vol. 16, No. 6, pp. 1016–1024.
- Zia, H. and Lecampion, B., 2017. "Propagation of a height contained hydraulic fracture in turbulent flow regimes". *International Journal of Solids and Structures*, Vol. 110-111, pp. 265–278. ISSN 00207683. doi: 10.1016/j.ijsolstr.2016.12.029.

7. RESPONSIBILITY NOTICE

The authors are solely responsible for the printed material included in this paper.